Брэгг-Френелевская оптика

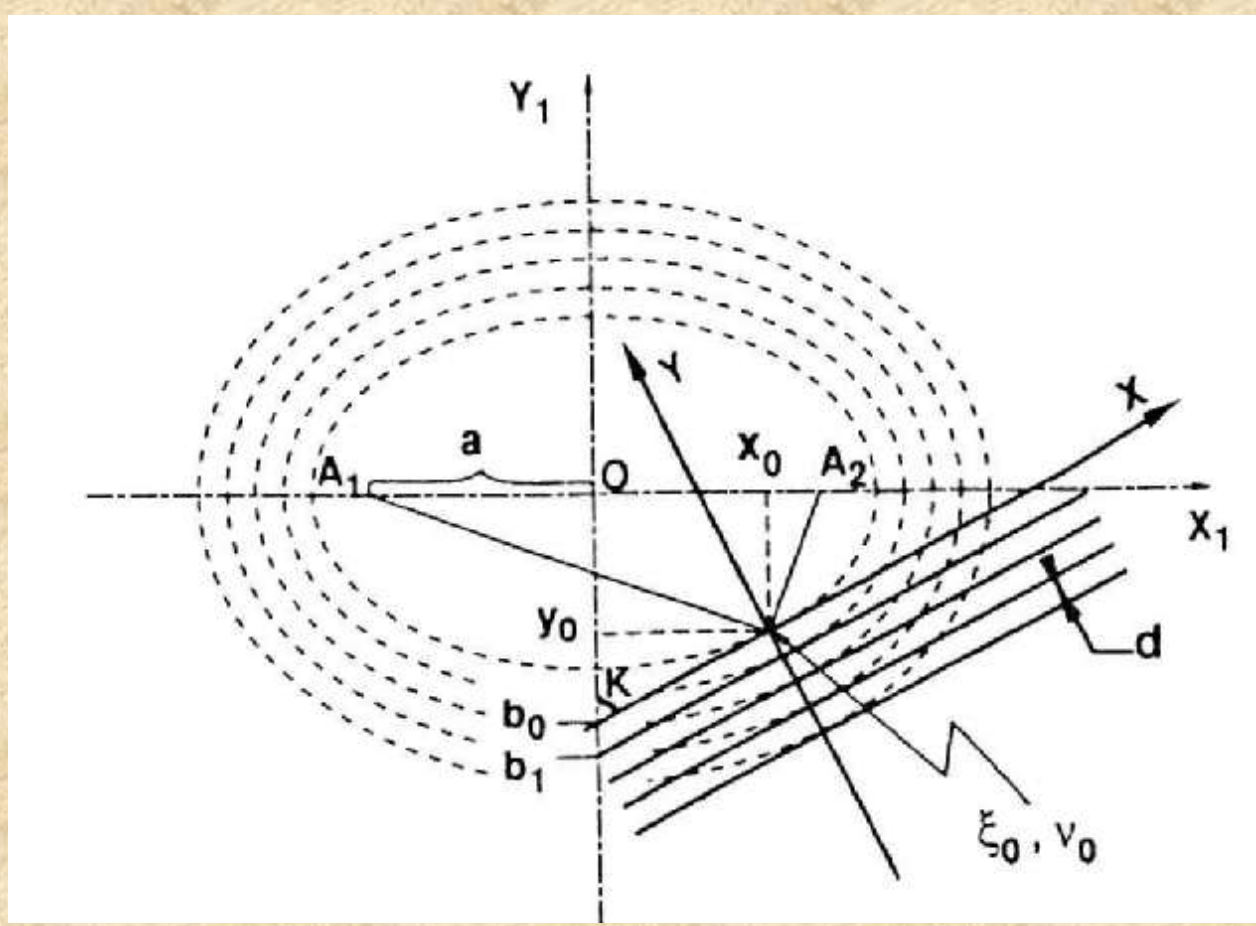

Брэгг-Френелевская оптика

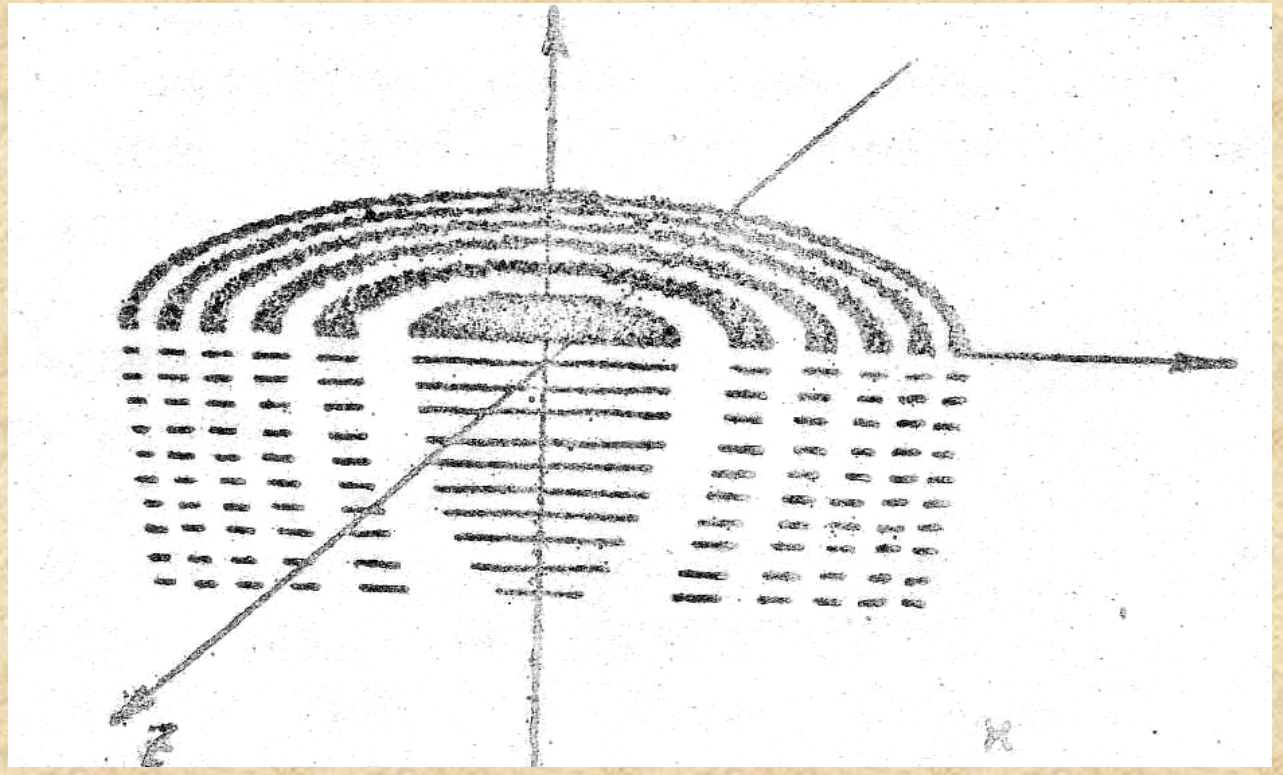

Брэгг-Френелевская оптика

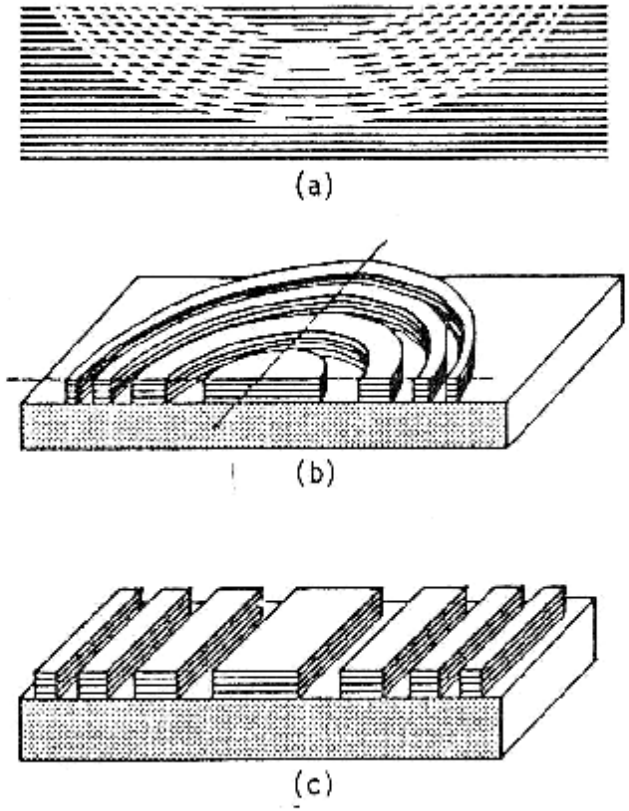

Fig. 2. (a) Scheme of a BFMFE free from spherical aberrations, (b) section of a practical BFMFE having a rectangular profile and capable of providing point focusing, (c) section of a practical BFMFE having a rectangular profile and providing linear focusing.

Брэгг-Френелевская оптика

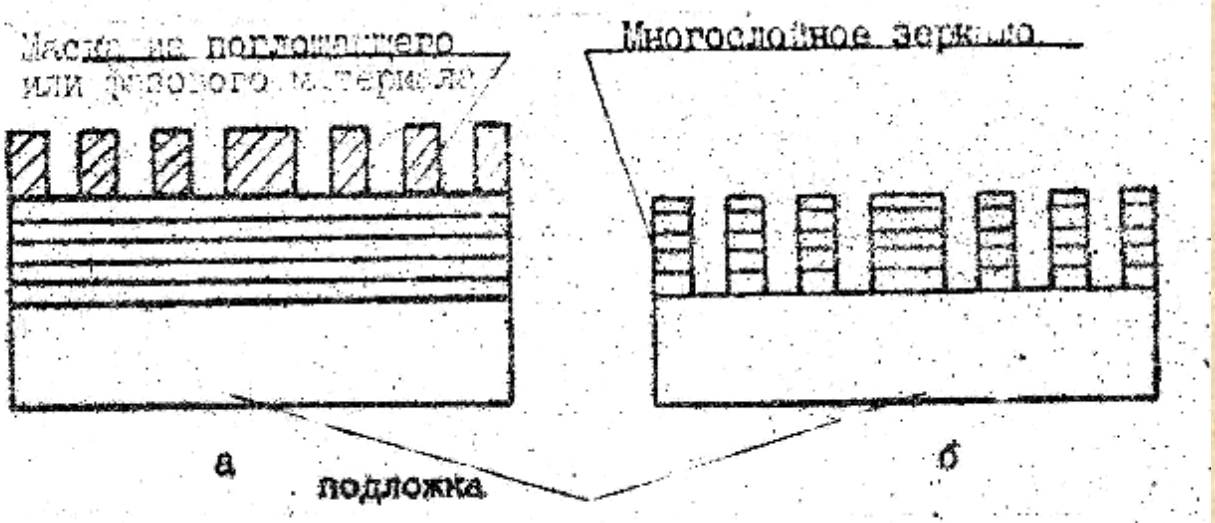

Рис.9. Формирование амплитудно-фазовых БФЛ: а - с помощью маски из амплитудно- фазового материала, б - с помощью травления многослойной структуры.

Брэгг-Френелевская оптика

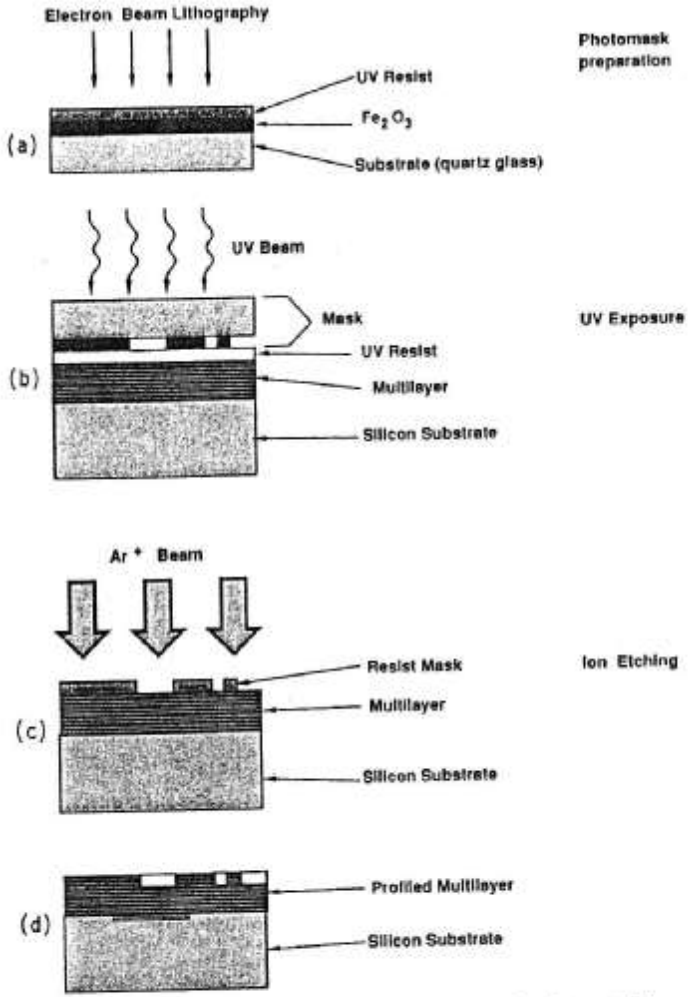

Fig. 4. Scheme of the BFMFE fabrication by ion etching of multilayers: (a) UV photomask preparation by electron beam writing on photoresist, (b) UV exposure for mask reproduction on the multilayer photoresist, (c) ion etching of the multilayer, (d) obtained BFMFE structure with a rectangular profile.

Брэгг-Френелевская оптика

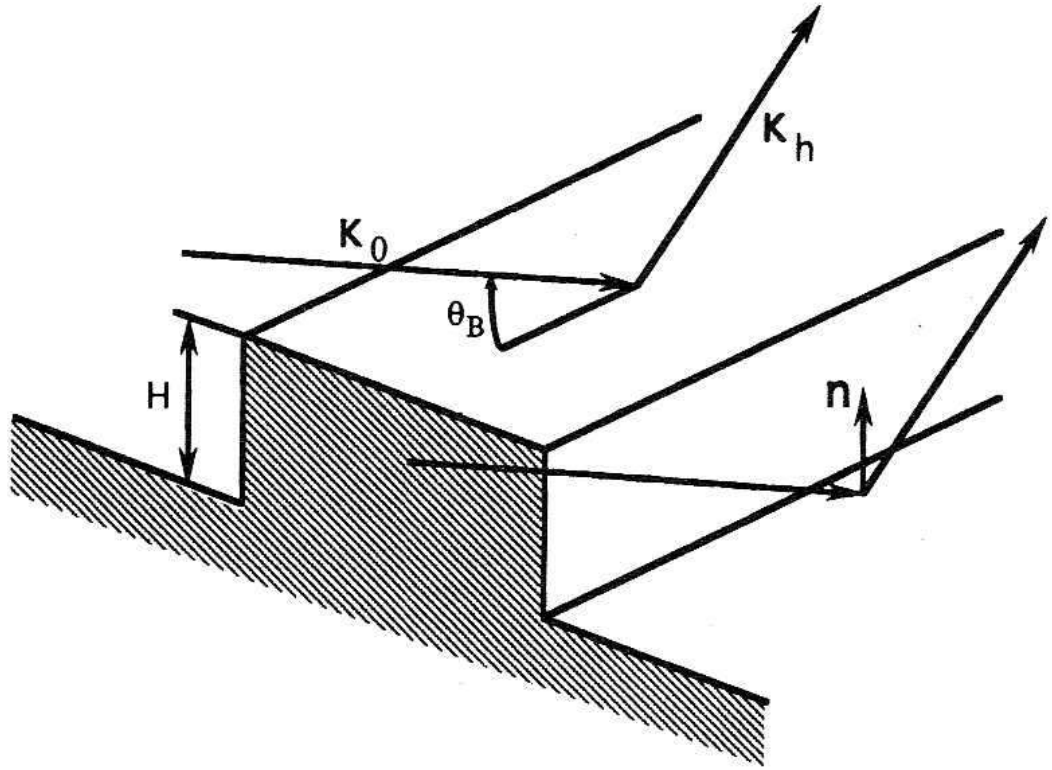

FIG. 1. Sketch illustrating the sagittal focusing with diffraction from a rectangular profile of crystal surface.

Брэгг-Френелевская оптика

$$\Delta\phi = 2\pi h(\chi_0 + \alpha \sin 2\theta_B)/(\lambda \sin \theta_B), \quad (3)$$

and it is thus linearly dependent on α. Therefore, by deviating a crystal-lens from the exact Bragg position, one can control the wave phase shift, without changing the BFL zone relief height. In this case intensity oscillations are observed at the focal spot, their period being determined by the expression

$$\alpha_p = \lambda/(2h\cos \theta_B), \quad (4)$$

which is $\alpha_p = 9.2''$ in our case.

Брэгг-Френелевская оптика

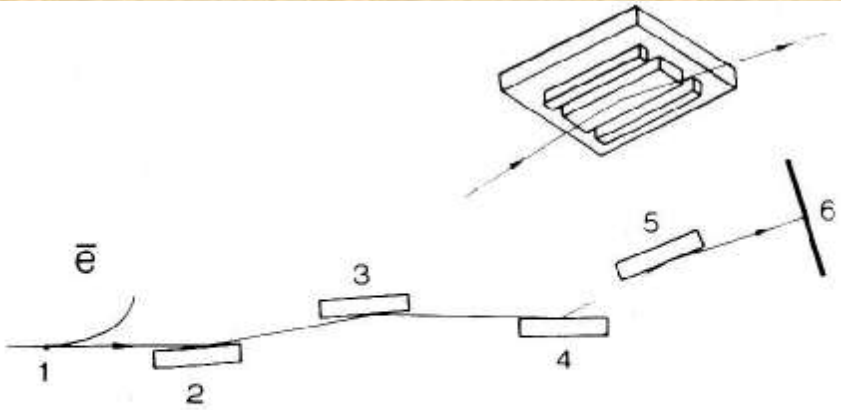

Fig. 2. Experimental layout: (1) X-ray source, (2,3) double crystal-monochromator, (4) asymmetric crystal-monochromator, (5) BFL, (6) observation plane.

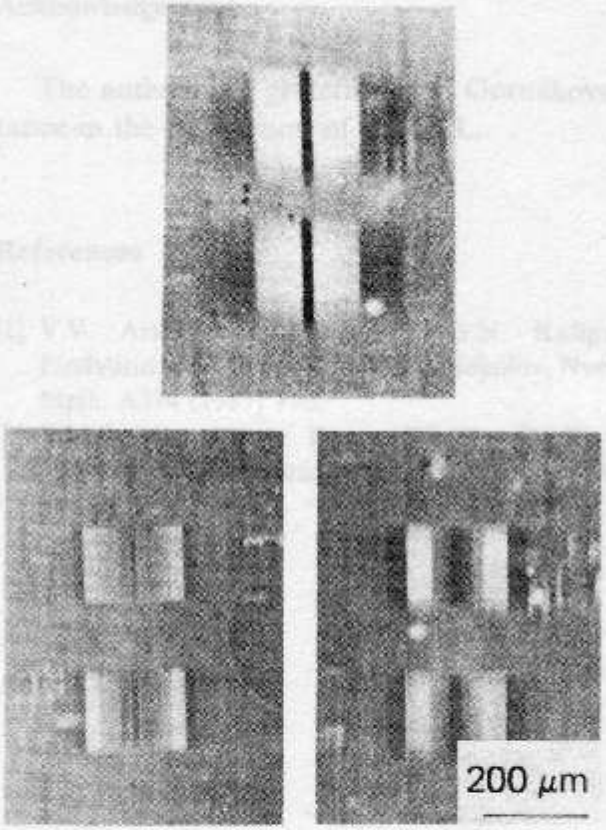

Fig. 3. Experimental topographs obtained according to the layout shown in fig. 2 by means of varying the BFL-observation plane distance: below left: 25 cm, below right: 50 cm, top: 98 cm.

Брэгг-Френелевская оптика

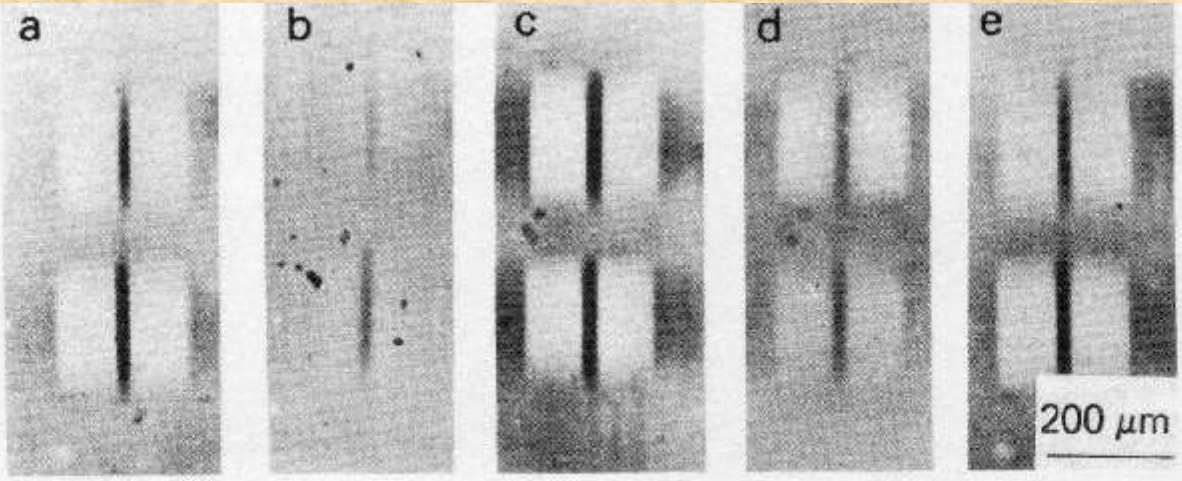

Fig. 4. Experimental topographs obtained using the layout shown in fig. 2 upon deviation of the crystal-lens from the exact Bragg position: (a) −10″, (b) −5″, (c) 0″, (d) +5″, (e) +10″.

Брэгг-Френелевская оптика

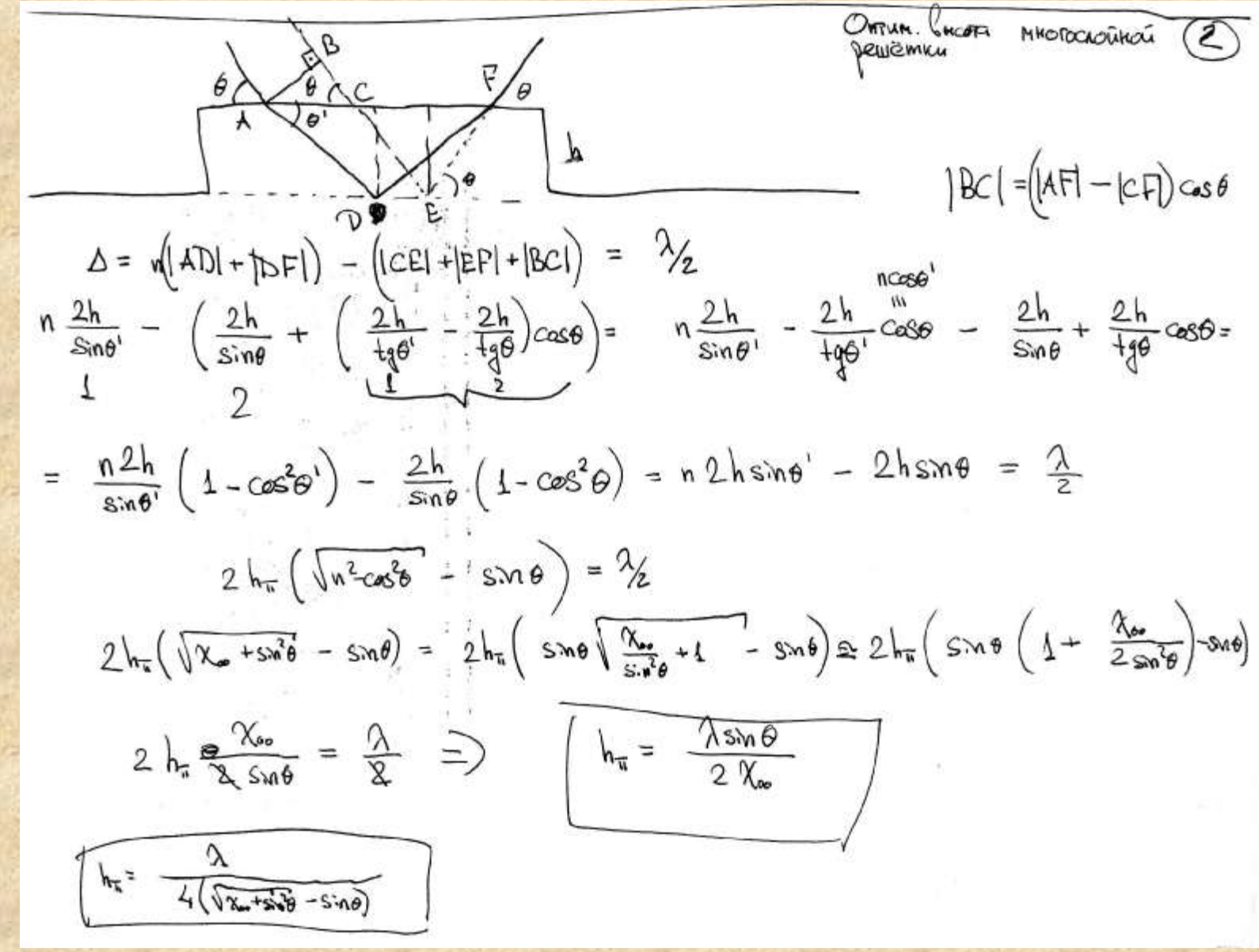

Брэгг-Френелевская оптика

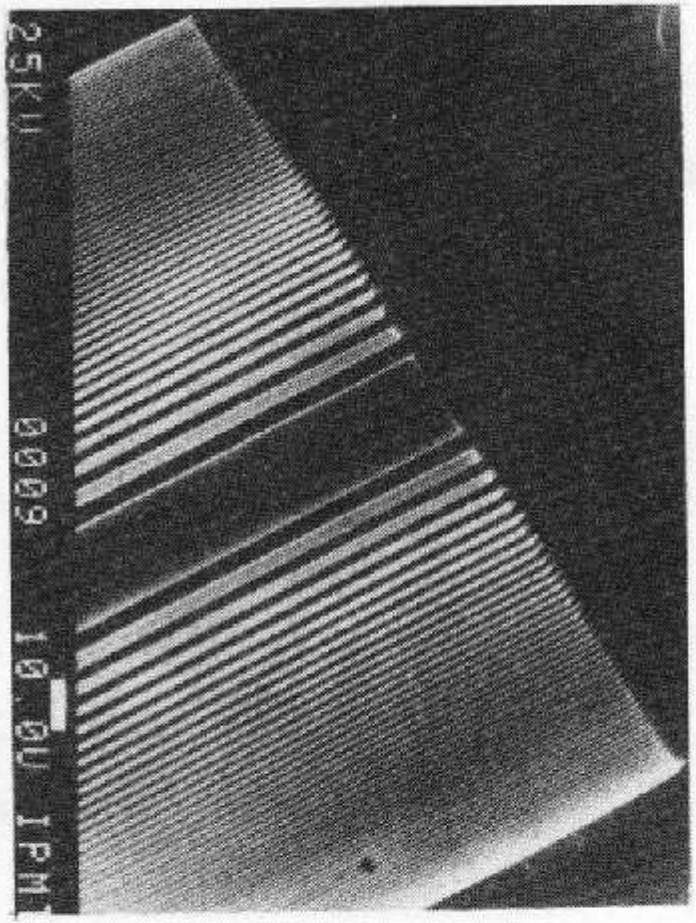

Fig.1. Typical linear phase BFL structure

Брэгг-Френелевская оптика

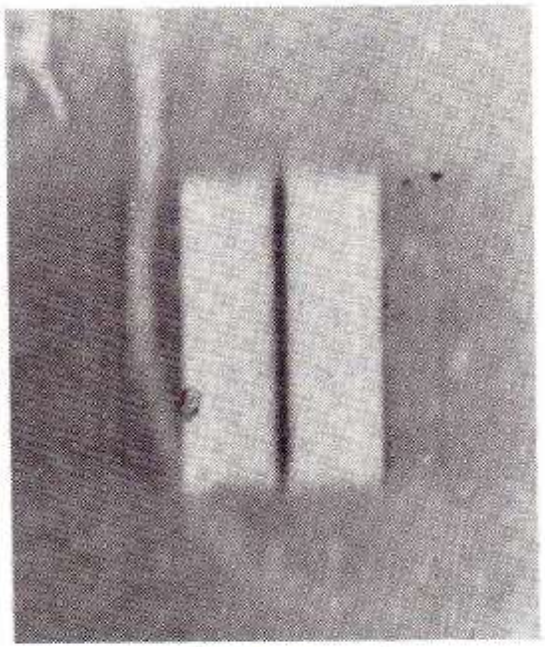

200 μm

a)

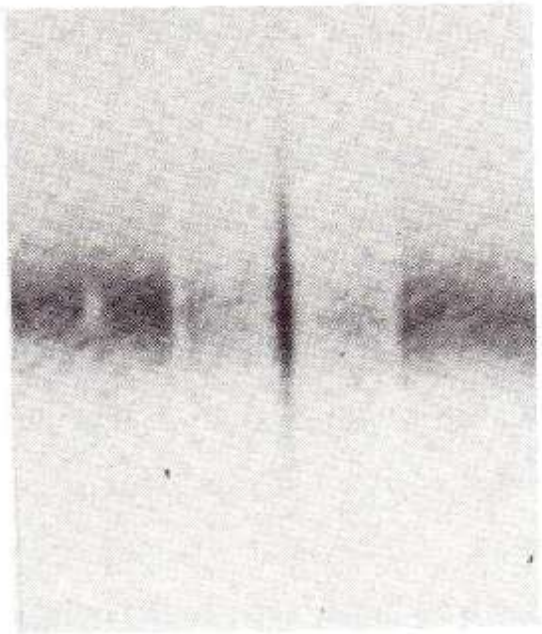

100 μm

b)

Fig 1. Linear focusing of (a) SR with E = 10 keV (b) CuK_{α} radiation.

Брэгг-Френелевская оптика

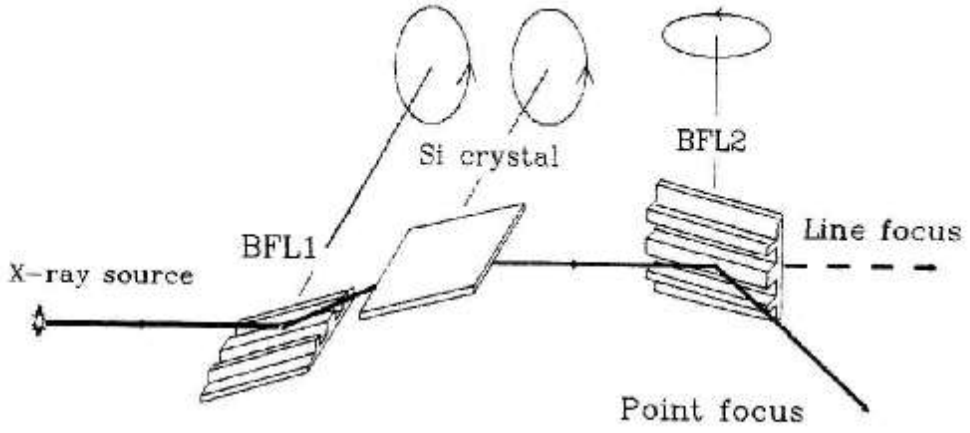

Layout parameters

BFL1 focal length – 15 cm
BFL2 focal length – 10 cm
Si(111) flat crystal
Microfocus X-ray generator with
Cu anode

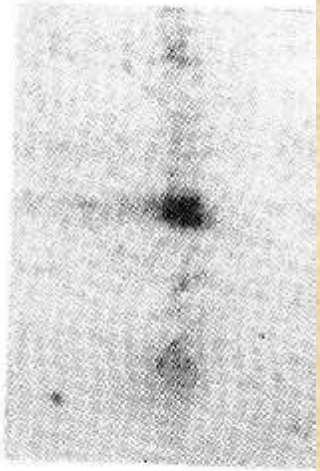

Fig.3. Schematic of the triple crystal X-ray microprobe.

Брэгг-Френелевская оптика

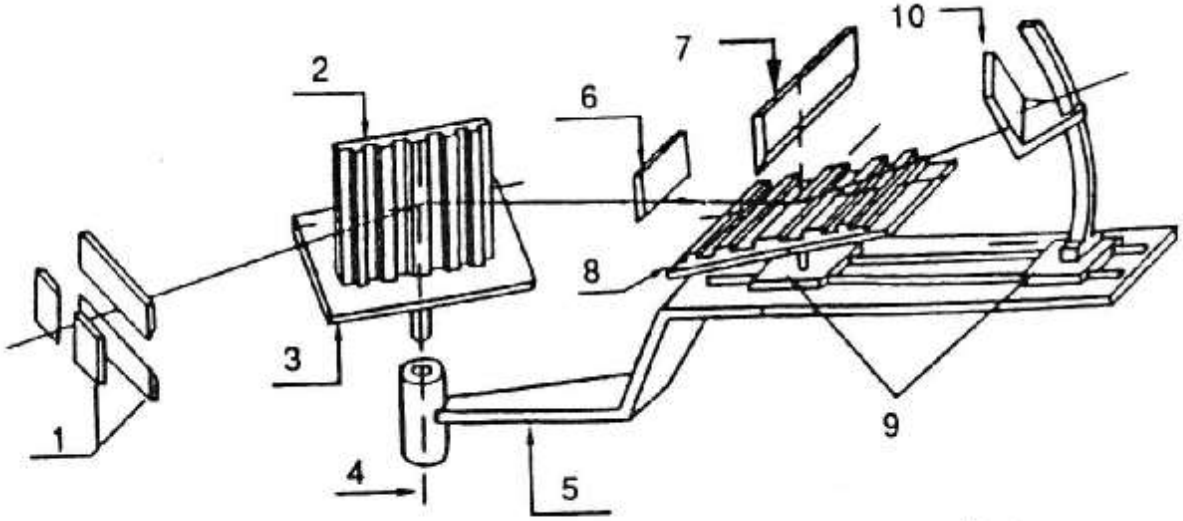

1. Input slit
2. BFMFE 1
3. BFMFE 1 stage
4. Axis of rotation
5. Goniometer
6,7. Slits
8. BFMFE 2
9. BFMFE 2 stage
10. Recording plate

Fig. 5. Scheme of the experimental setup.

Брэгг-Френелевская оптика

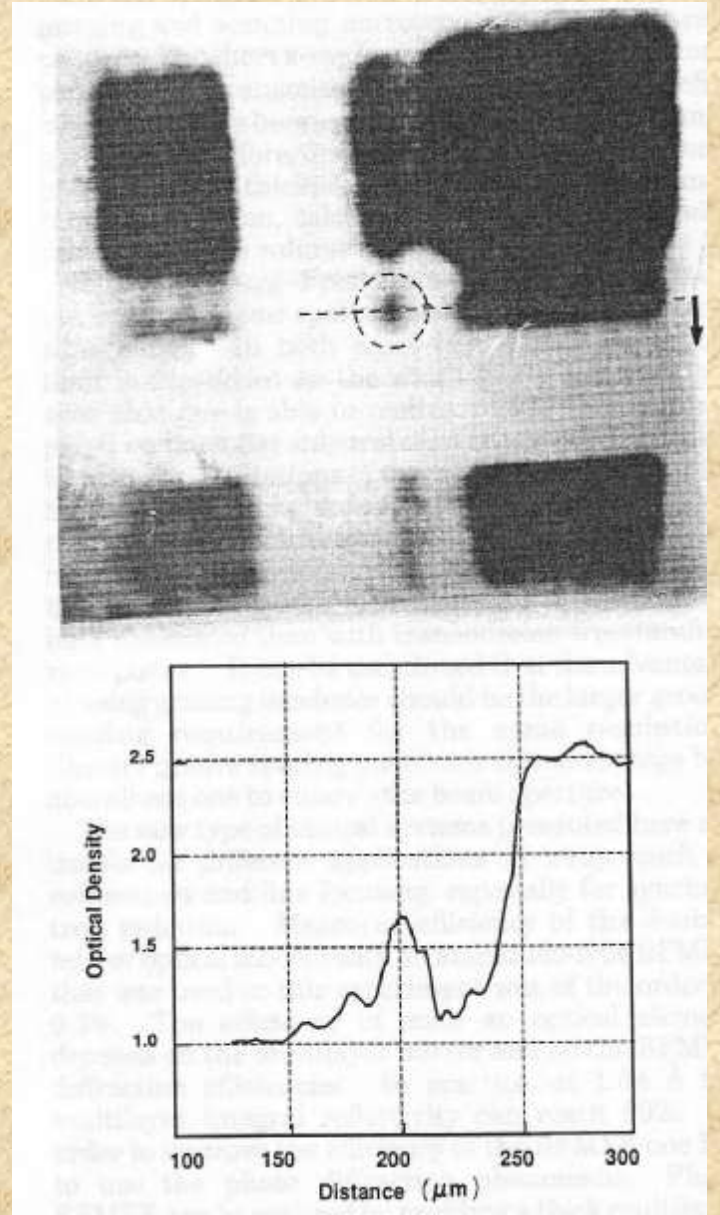

Брэгг-Френелевская оптика

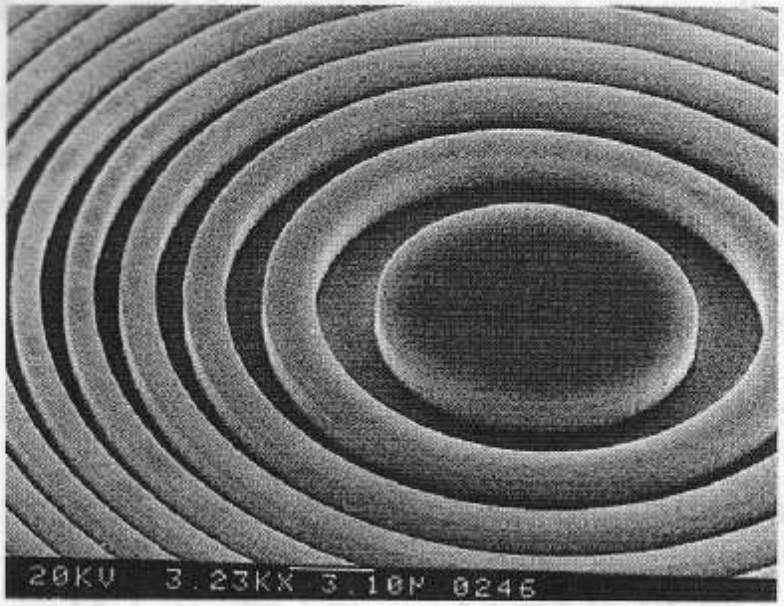

Fig. 2. Image of the Ge Bragg-Fresnel lens obtained from Scanning Electron Microscope. Innermost zone radius $r_1 = 3.9$ μm, outermost zone width $\Delta r_n = 0.15$ μm, aperture $A = 100$ μm, zone height $h = 2$ μm.

Брэгг-Френелевская оптика

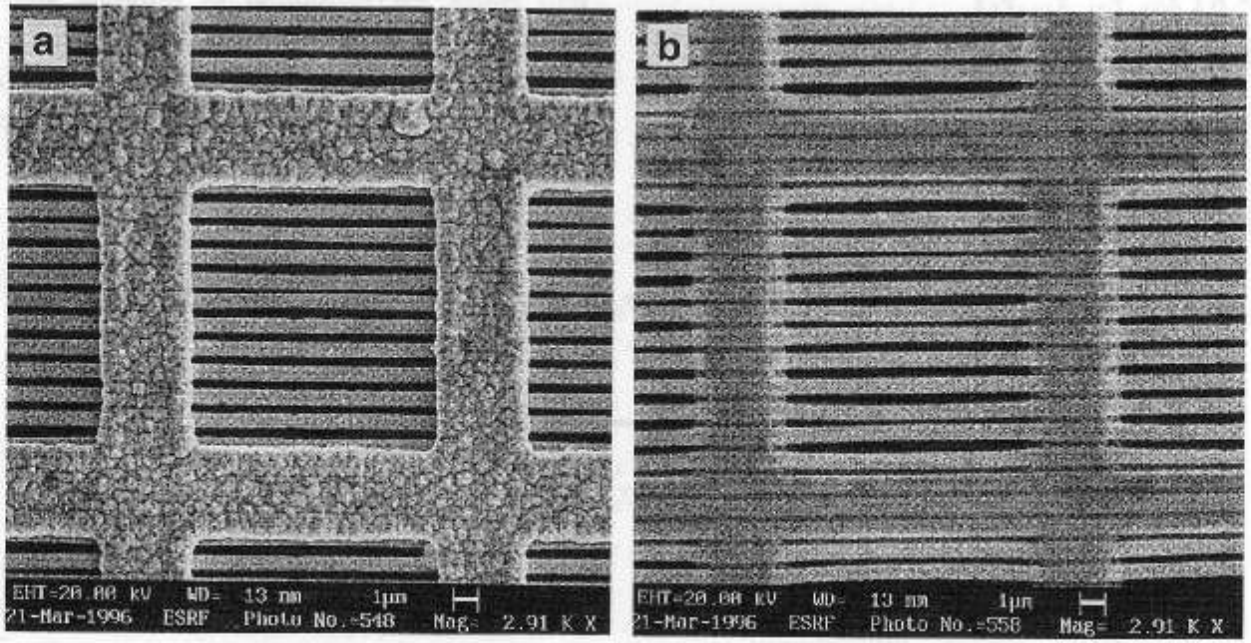

Fig. 3. SEM micrograph of the test object from the front (a) and back (b) sides used for X-ray imaging: gold grid with 0.5 μm feature supported by free-standing gold mesh with pitch size of 15 μm and bars of 3 μm.